Effect of uniform distributions of bonded and debonded fibers on the growth of the fiber/matrix interface crack in UD laminates with different fiber contents under transverse loading

Luca Di Stasio[a,b], Janis Varna[b], Zoubir Ayadi[a]

[a] *Université de Lorraine, EEIGM, IJL, 6 Rue Bastien Lepage, F-54010 Nancy, France*
[b] *Luleå University of Technology, University Campus, SE-97187 Luleå, Sweden*

Abstract

Priority: 1

Target journal(s): Composites Part B: Engineering, Composites Part A: Applied Science and Manufacturing, Composite Structures, Journal of Composite Materials, Composite Communications

1. Introduction

1. We start with a few lines devoted to the spread tow technology and thin plies: what they are, what can be done, what are the possible applications.
2. By quoting the relevant references, we report on the observation that one of the main beneficial mechanisms in thin ply is the retardation of transverse crack propagation. We then enlarge by reporting the microscopical observations by Saito, in which debonds where also observed. We observe that available microscopic observations are just a few and mainly in 2D.
3. Propagation of transverse cracks has been widely investigated both analytically and numerically
4. Initiation at the level of fiber/matrix interface is instead a less researched subject.

5. cohesive elements are a possible choice, but have some drawbacks, which makes a LEFM approach valuable
6. With regard to LEFM studies of laminates under transverse loading, models can be found in the literature about: the single fiber in infinite matrix under different mode of loading, the effect of adjacent fibers on a fiber in infinite matrix under different mode of loading, the single fiber in an equivalent composite in transverse tension, the effect of adjacent fibers on a fiber in an equivalent composite in transverse tension.
7. For initiation of transverse cracking at the fiber/matrix interface in UD laminates under transverse tension, there is thus a gap regarding: the effect of fiber volume fraction; the interaction of debonded and bonded fibers in micro-structured assemblies, i.e. no homogenization. This article addresses these two points.
8. We conclude the introduction with a summary of the article's structure.

2. RVE models & FE discretization

2.1. Models of Representative Volume Element (RVE)

In order to investigate the interaction between debonds in UD laminates, we developed different models of laminates in which the only damage present is represented by the fiber/matrix interface crack. All of these Representative Volume Elements feature regular microstructures with fibers placed according to a square-packing tiling. Laminates are considered to be plane and infinite to all practical purposes in their own plane, i.e. along laminate axes x and y. This allows the use of 2D models under the assumption of plane strain, defined in the $x - z$ section of the laminate. Consequently, debonds are considered to be fully developed along the length of the respective fiber, corresponding to the y laminate axis or laminate's width, but only partially along the surface of the fiber, i.e. the circumferential direction. The analysis presented thus applies to long debonds, of which we interested in understanding the mechanism of growth along the surface of the fiber. Laminates are further supposed to be subjected to transverse tension, applied along the x direction in the pictures. The first two models feature, as shown in Fig. 1, a UD laminate with only one layer of fibers across its thickness. This is quite an extreme model from the microstructural point of view, however it allows to focus the analysis on the interaction between debonds placed along the direction of the load. In retrospective, if only 20 years ago such a model would have been considered too abstracted from the physical reality, the recent advancements in the spread tow technology make this approach appealing also for practical considerations. In the first version of the model, Subfig 1a, debonds appear in the laminate every m fibers

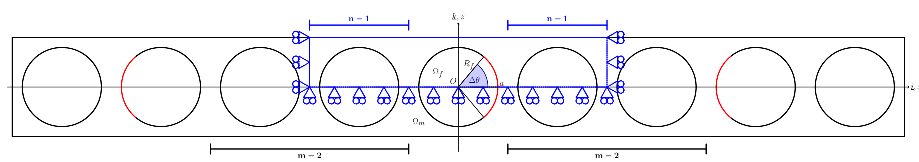

(a) Single layer of fibers with a debond appearing every m fibers.

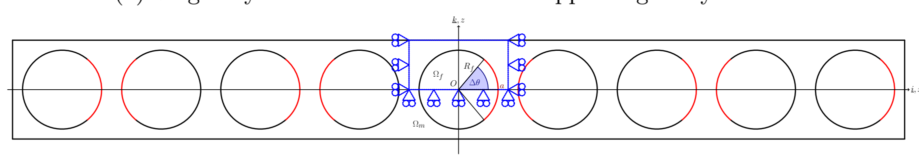

(b) Single layer of fibers with debonds appearing on each fiber.

Figure 1: Models of UD laminates with a single layer of fibers and debonds repeating at different distances. The corresponding repeating element (RVE) is highlighted in blue.

2.2. Finite Element (FE) discretization

We describe the model implemented: schematic + description of parameters, formulation (LEFM, frictionless contact, VCCT, J-Integral), implementation of BCs, mesh. Fig. 3

2.3. Validation of the model

We mention once in this paper the validation of the model with respect to BEM results. Fig. 4

3. Results & Discussion

3.1. Effect of Fiber Volume Fraction

The effect is similar for all the different BC cases, it's enough to show some of them to exemplify. G_I in Fig. 5, G_{II} in Fig. 6.

Graphics of ERR vs $\Delta\theta$, one curve for each V_f, one graphic for each selected BC. Selected BC: free, coupling, some examples with fibers (see captions).

3.2. Interaction between debonds in UD laminates with a single layer of fibers

We start with a simpler (1 parameter: number of fibers in the horizontal directions) but more extreme model: one line of fibers. What's the effect on G_I and G_{II}? It increases them: a compliant element in the middle of two stiffer ones. Reference to Kies strain magnification. G_I in Fig. 7, G_{II} in Fig. 8.

One graphic for each V_f (30%,50%,60%,65%), one curve for each case of fibers on the side (1, 2, 3, 5, 10, 50, 100).

3.3. Influence of layers of fully bonded fibers on debond's growth in a centrally located line of debonded fibers

We then move to a ply with multiple lines of fibers and only debonded fibers in the central one (still only 1 parameter: number of fibers in vertical direction, but bit closer to real plies). No significant effect. G_I in Fig. 9, G_{II} in Fig. 10.

One graphic for each V_f (30%,50%,60%,65%), one curve for each case of fibers on top (1, 2, 3, 5, 10, 50, 100).

3.4. Interaction between debonds in UD laminates with multiple layers of fibers

Finally models that are closer to real laminates and are more complex (2 parameters: number of fibers along the horizontal direction, number of layers in the vertical one). G_I in Fig. 11, G_{II} in Fig. 12.

One graphic for each V_f (30%,50%,60%,65%), one curve for some selected case of fibers on top and on the side. Hypothesis of selected cases ([n. on side,

n. on top]): [1,1], [2,1], [2,2], [5,1], [5,5], [10,1], [10,10], [50,1], [50,10], [100,1], [100,10]

3.5. Comparison with the single fiber model with equivalent boundary conditions

We compare the previous results with the corresponding models of single fibers with equivalent BC. We draw conclusions on the possibility of using a single fiber with equivalent BCs. By remembering the actual ply configurations the repeating elements are modeling, and observing that in the vertical direction no significant effect related to the presence of debonded or bonded fiber can be found, we conclude that debonds appearing in fibers aligned in the vertical direction are energetically equivalent, and thus different configurations of debonded/bonded fibers along the vertical direction have the same probability. It is thus likely, from the energetic point of view, that debonds form at the same time along fibers aligned vertically. G_I in Fig. 13 and Fig. 15, G_{II} in Fig. 14 and Fig. 16.

One graphic for each V_f (30%,50%,60%,65%), one curve for single fiber with BC + some selected case of fibers on top and on the side. Hypothesis of selected cases ([n. on side, n. on top]): [1,1], [2,1], [2,2], [5,1], [5,5], [10,1], [10,10]

4. Conclusions & Outlook

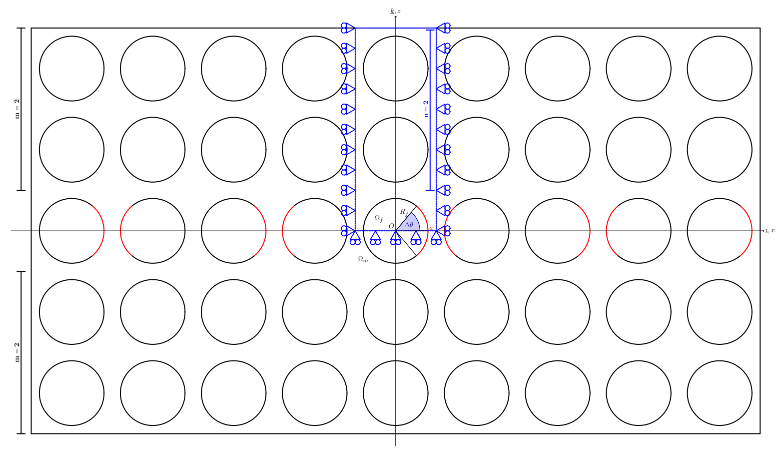

(a) Multiple layers of fibers with debonds appearing on each fiber beloging to the central layer.

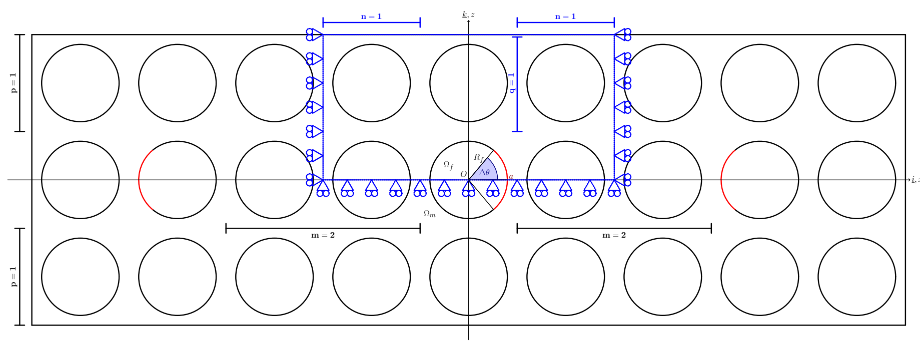

(b) Mutiple layers of fibers with a debond appearing every m fibers within the central layer.

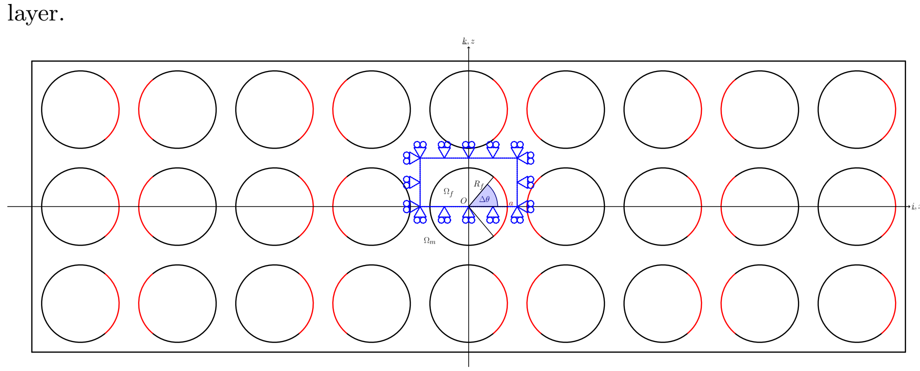

(c) Multiple layers of fibers with debonds appearing on each fiber.

Figure 2: Models of UD laminates with different layers of fibers and debonds repeating at different distances. The corresponding repeating element (RVE) is highlighted in blue.

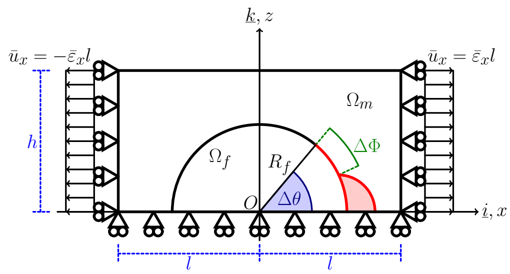

(a) Schematic of the model with its main parameters.

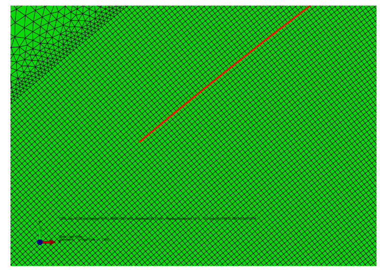

(b) Detail of the mesh in the crack tip's neighborhood.

Figure 3: Details and main parameters of the Finite Element model.

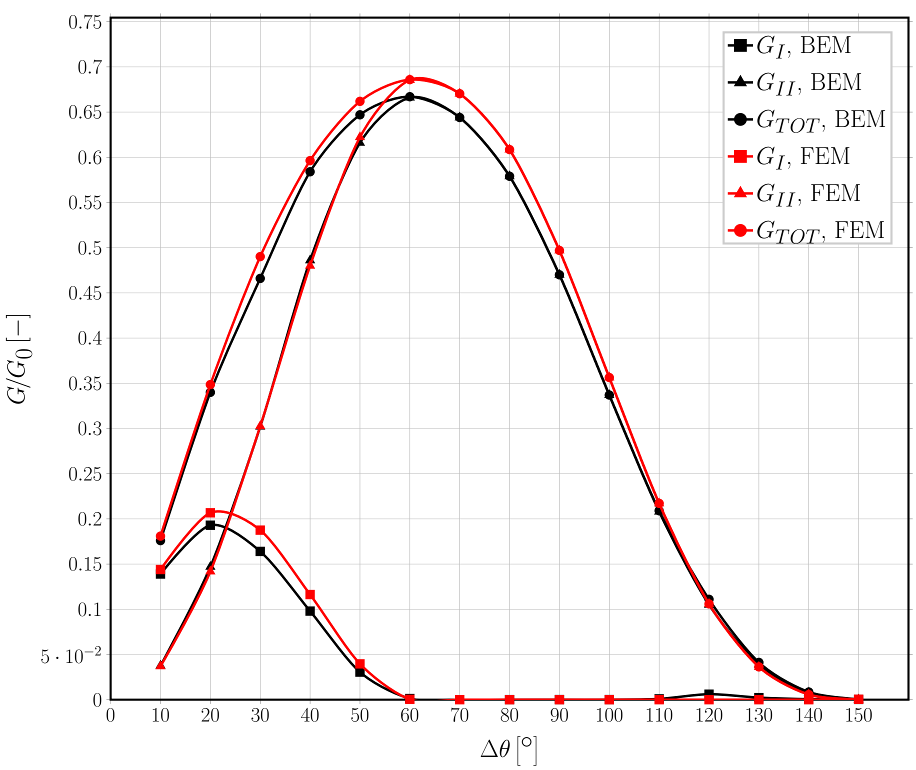

Figure 4: Validation of the single fiber model for the infinite matrix case with respect to the BEM solution in [].

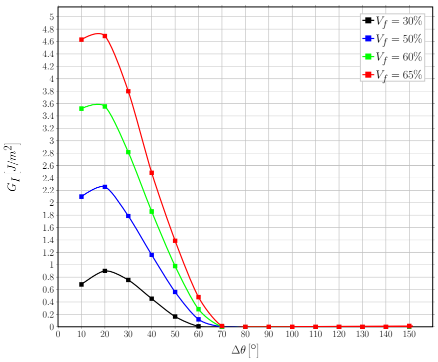

(a) 5 fibers each side, 5 above.

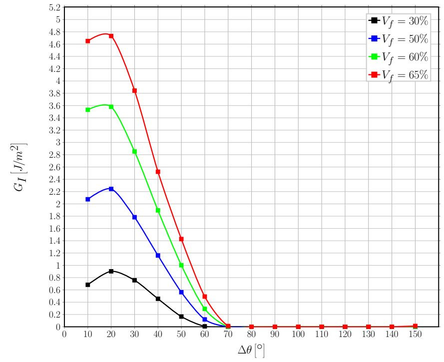

(b) 10 fibers each side, 10 above.

Figure 5: A view of the effect of fiber volume fraction on Mode I ERR in two exemplificative models.

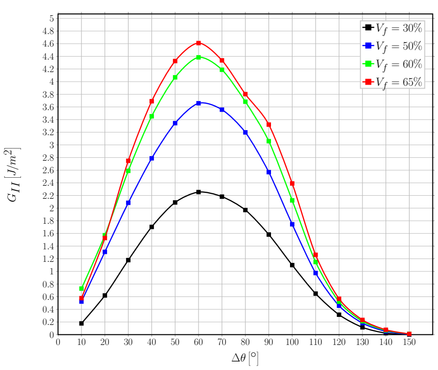

(a) 5 fibers each side, 5 above.

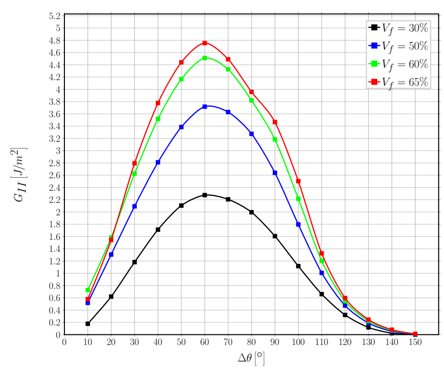

(b) 10 fibers each side, 10 above.

Figure 6: A view of the effect of fiber volume fraction on Mode II ERR in two exemplificative models.

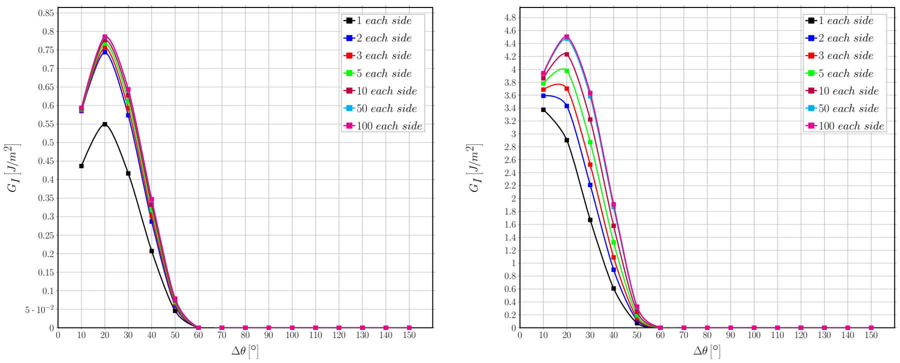

(a) $V_f = 30\%$.

(b) $V_f = 60\%$.

Figure 7: Effect of the interaction between debonds appearing at regular intervals on Mode I ERR in a single-ply laminate with a single layer of fibers at different levels of fiber volume fraction V_f.

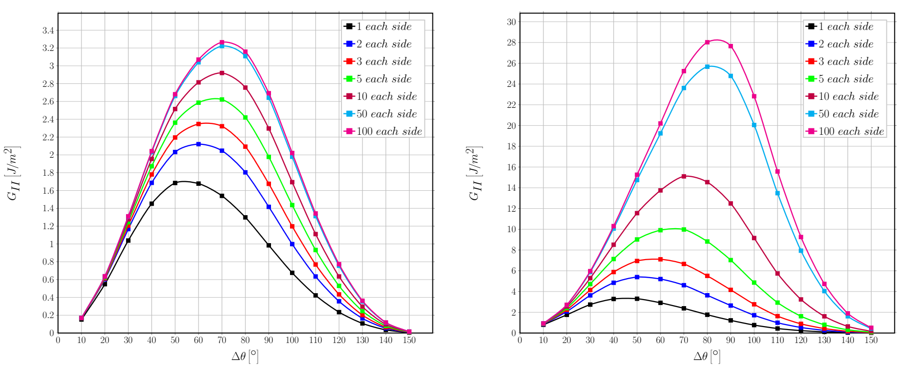

(a) $V_f = 30\%$.

(b) $V_f = 60\%$.

Figure 8: Effect of the interaction between debonds appearing at regular intervals on Mode II ERR in a single-ply laminate with a single layer of fibers at different levels of fiber volume fraction V_f.

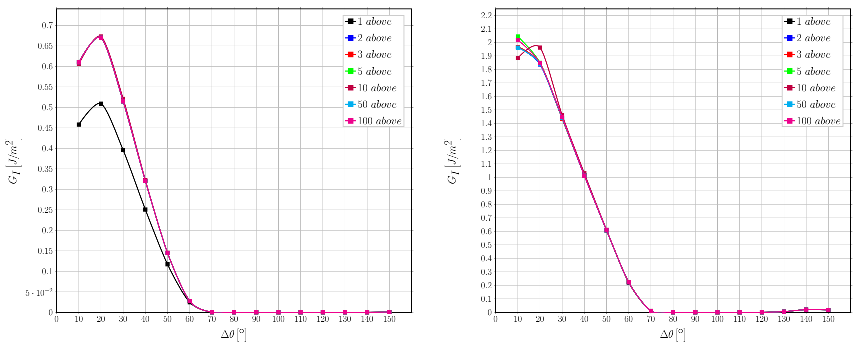

(a) $V_f = 30\%$.

(b) $V_f = 60\%$.

Figure 9: Influence of layers of fully bonded fibers on debond's growth in Mode I ERR in a centrally located line of debonded fibers at different levels of fiber volume fraction V_f.

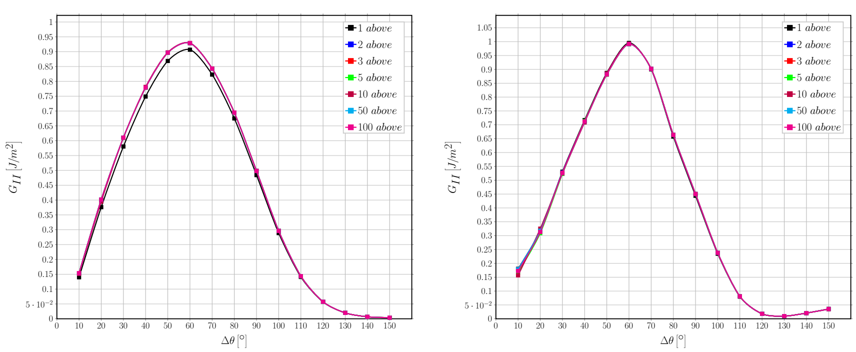

(a) $V_f = 30\%$.

(b) $V_f = 60\%$.

Figure 10: Influence of layers of fully bonded fibers on debond's growth in Mode II ERR in a centrally located line of debonded fibers at different levels of fiber volume fraction V_f.

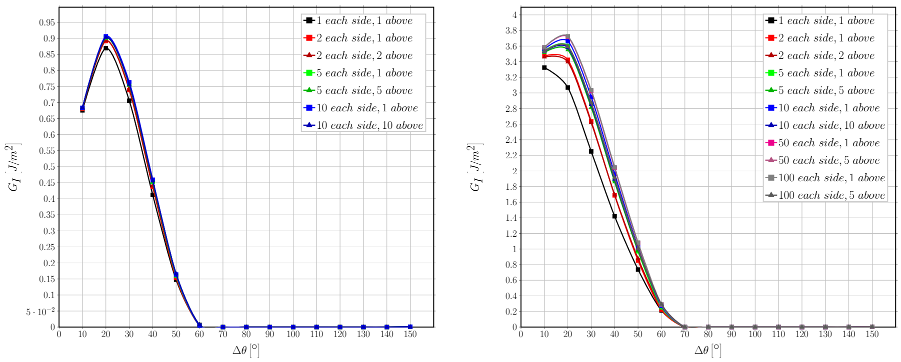

(a) $V_f = 30\%$.

(b) $V_f = 60\%$.

Figure 11: Effect of the interaction between debonds appearing at regular intervals on Mode I ERR in a single-ply laminate with multiple layers of fibers at different levels of fiber volume fraction V_f.

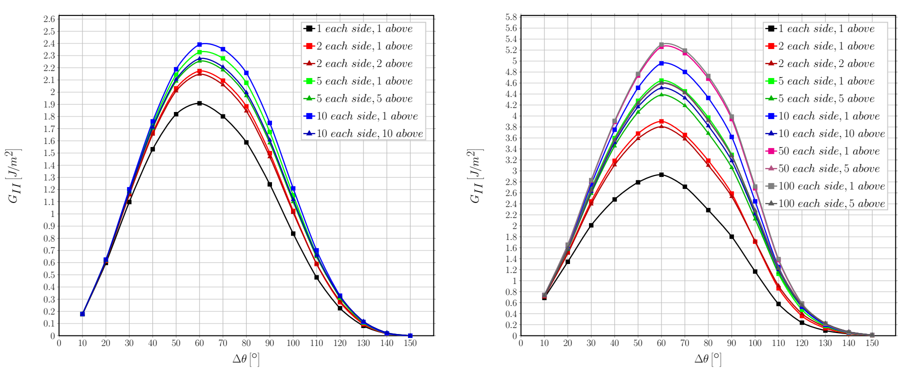

(a) $V_f = 30\%$.

(b) $V_f = 60\%$.

Figure 12: Effect of the interaction between debonds appearing at regular intervals on Mode II ERR in a single-ply laminate with multiple layers of fibers at different levels of fiber volume fraction V_f.

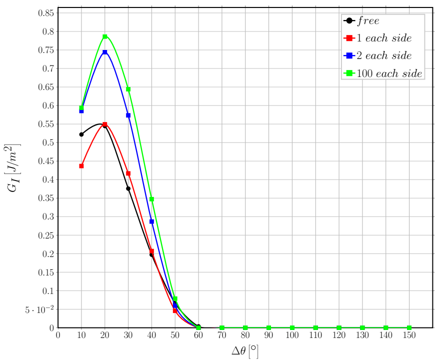

(a) $V_f = 30\%$.

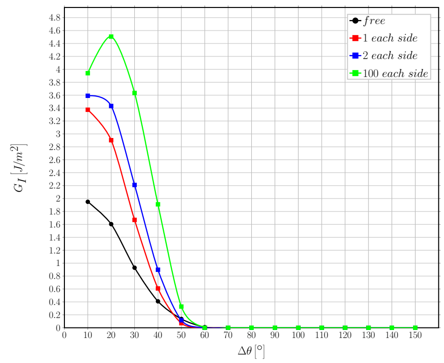

(b) $V_f = 60\%$.

Figure 13: Comparison of Mode I ERR between the single fiber model with free upper boundary and the multiple fibers model with fibers only on the side at different levels of fiber volume fraction V_f.

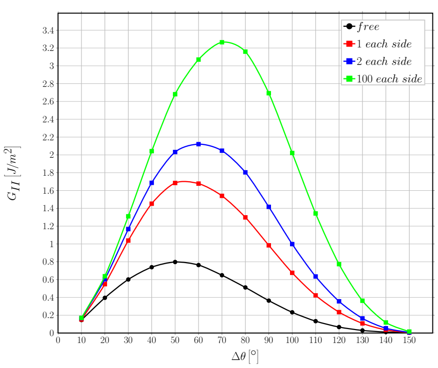

(a) $V_f = 30\%$.

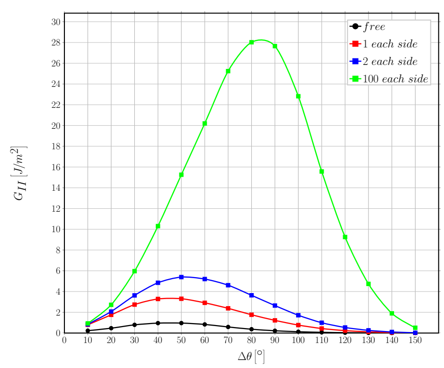

(b) $V_f = 60\%$.

Figure 14: Comparison of Mode II ERR between the single fiber model with free upper boundary and the multiple fibers model with fibers only on the side at different levels of fiber volume fraction V_f.

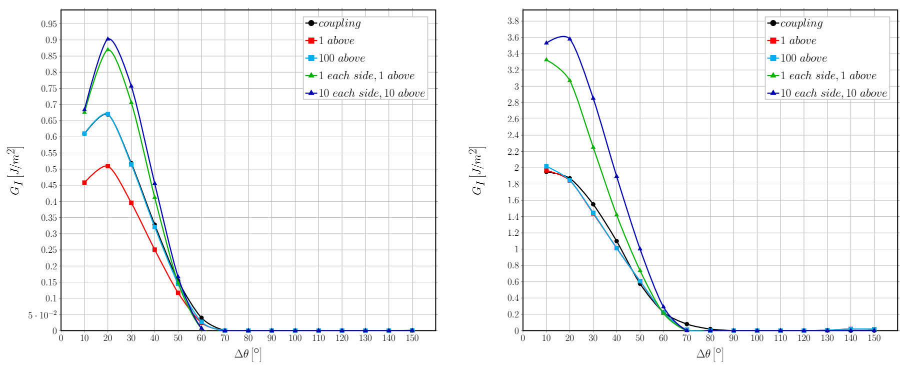

(a) $V_f = 30\%$.

(b) $V_f = 60\%$.

Figure 15: Comparison of Mode I ERR between the single fiber model with coupling conditions along the upper boundary and the multiple fibers model with fibers above and both above and on the side at different levels of fiber volume fraction V_f.

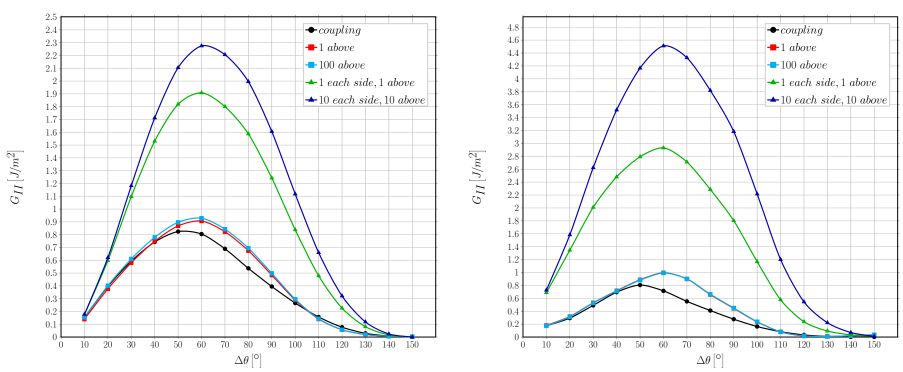

(a) $V_f = 30\%$.

(b) $V_f = 60\%$.

Figure 16: Comparison of Mode II ERR between the single fiber model with coupling conditions along the upper boundary and the multiple fibers model with fibers above and both above and on the side at different levels of fiber volume fraction V_f.